Available online at www.sciencedirect.com
SCIENCE DIRECT®
Thermochimica Acta 429 (2005) 73–79
thermochimica acta
www.elsevier.com/locate/tca

Thermal diffusivity of eutectic of alkali chloride and ice in the freezing–thawing process by temperature wave analysis

N.J. Chen[a,1], J. Morikawa[a], A. Kishi[b], T. Hashimoto[a,*]

[a] *Graduate school of Science and Engineering, Tokyo Institute of Technology, 2-12-1 Ohokayama, Meguro-ku, Tokyo 152-8552, Japan*
[b] *Rigaku Corporation, 3-9-12 Matsubara-cho, Akishima, Tokyo 196-8666, Japan*

Received 1 September 2004; received in revised form 26 October 2004; accepted 3 November 2004
Available online 4 January 2005

Abstract

Thermal diffusivity of eutectic formed in aqueous alkali chloride solutions (NaCl, KCl, RbCl and CsCl) was determined by temperature wave analysis (TWA) during the freezing–thawing process of aqueous alkali chloride solution. An obvious change of thermal diffusivity in freezing–thawing processes of eutectic was observed with the super-cooling phenomena for each alkali chloride solute. The rate of thermal diffusivity decrease during the eutectic melting in comparison to the total decrease from the solid to the liquid state was observed larger than that of the heat of fusion measured by DSC, especially in the dilute concentration. It was confirmed that thermal diffusivity was sensitively influenced by the highly structure of the coexistence of eutectic crystallization and ice.

Keywords: Temperature wave analysis; Freezing–thawing process; Thermal diffusivity; Alkali chloride; Eutectic

1. Introduction

Properties of electrolyte solutions, such as viscosity, diffusion coefficient, or electrical conductivity, have long been the subject of considerable attention and study [1,2]. However, for heat transport property, such as thermal diffusivity and thermal conductivity in the freezing temperature range, accurate data is still needed especially in the phase transition region. As we know, thermal diffusivity is defined as a transport coefficient of temperature, while thermal conductivity is that of heat energy. Thermal conductivity λ is related to thermal diffusivity α by the formula $\lambda = \alpha C$, where C is the specific heat per unit volume. To obtain these thermal transport properties, lots of methods were applied such as thermal wave transmission spectroscopy method [3–5], photopyroelectric technique [6–8], probe method [9], steady state method [10], transient hot-wire method [11,12], forced Rayleigh scattering method [13], temperature wave analysis technique [14–17] and so on.

Temperature wave analysis (TWA) is a method for detecting thermal diffusivity by measuring the phase shift of temperature wave. It has been largely applied to the study of thermal property of various materials [14–16]. It has also been shown that, under particular experimental conditions, the TWA method is a very sensitive technique, to observe the glass transition of polymer, the solid–solid transition of molecular crystals, and the solid–liquid transition of various kinds of materials. With this technique, the quantitative value of heat transport property can be obtained in the liquid, the solid states, and in the phase transition. This technique was also applied to detect the thermal diffusivity of pure water and aqueous solutions in the frozen and unfrozen state, and the continuous changing of thermal diffusivity was observed as a function of temperature [17].

Aqueous solutions of NaCl, KCl, RbCl and CsCl were known to form the eutectic in the frozen state, respectively [18]. For example, the aqueous solution of NaCl, which is

* Corresponding author. Tel.: +81 3 5734 2435; fax: +81 3 5734 2435.
E-mail addresses: ningjuan@o.cc.titech.ac.jp (N.J. Chen), toshimas@o.cc.titech.ac.jp (T. Hashimoto).
[1] Tel.: +81 3 5734 3093; fax: +81 3 5734 3093.

0040-6031/$ – see front matter © 2004 Elsevier B.V. All rights reserved.
doi:10.1016/j.tca.2004.11.010

the typical electrolyte and most relative to our lives, forms the eutectic of $NaCl{\cdot}2H_2O$ with the melting temperature at −21.7 °C. In this study, thermal diffusivity of the eutectic formed in aqueous alkali chloride solutions (NaCl, KCl, RbCl and CsCl) with the various concentrations was examined by temperature wave analysis. A measurement of X-ray diffractometer (XRD) equipped with differential scanning calorimetry (DSC) was also undertaken to study the structure of the mentioned eutectic crystallizations.

2. Samples and measurements

2.1. Samples

Solutes of alkali chloride, NaCl, KCl, RbCl and CsCl were obtained from Wako Pure Chemical Industries, Co. Ltd., with the purity of at least 99.99%. Aqueous solutions were prepared by dissolving the solutes in pure water with the concentration of 0.05, 0.10, 0.154, 0.5, 1.0, 2.0 and 4.0 molar per liter. The electric resistivity of pure water is 15 MΩ cm.

2.2. TWA measurements

2.2.1. Apparatus

The experimental set-up used in this study is shown in Fig. 1. A set of flat plate of Pyrex 7740, sputtered with thin gold layers across an area of 1 mm × 3 mm with an electrical insulation coating on the surface, one for a heater on the front surface of the specimen and the other for a sensor on the rear surface of the sample, were used as measurement cell for thermal diffusivity (Fig. 1a). The electrical insulation coating, such as silicone oxide, is hydrophilic and the interfacial thermal resistance between this coating and the aqueous solution sample is assumed negligible, so the lubricant was not used in this study. This hypothesis is also confirmed for the measurement of phase shift at the thermal interface at least in the lower frequency by Minakov et al. [5]. To avoid the evaporation, the liquid specimen is inserted into the set of measurement cell fixed and sealed at a constant thickness with a spacer by using a capillary action. It was confirmed experimentally that the temperature variation obtained by a thermocouple buried in the substrate was less than 0.2 °C.

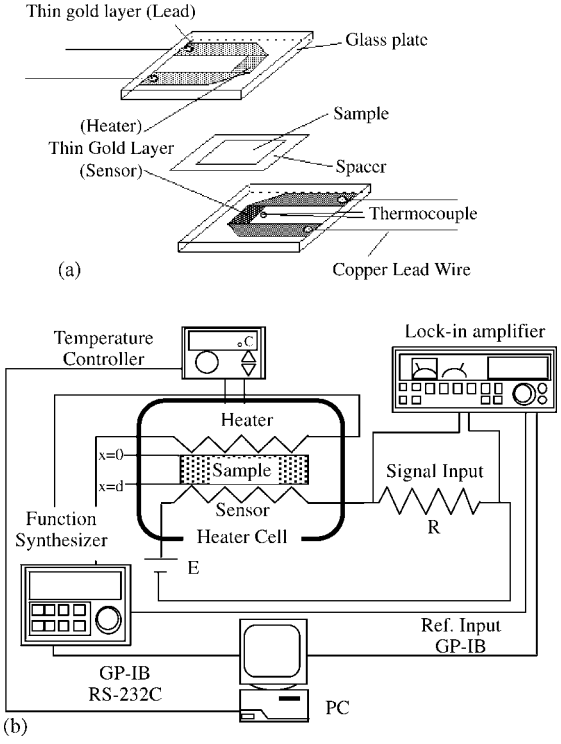

Fig. 1. Schematic diagram of the TWA measurement: (a) measurement cell; (b) experimental arrangement.

By passing a sinusoidal current on the heater by function synthesizer (NF1920), the temperature wave is generated by ac Joule heating at the front surface of the specimen and it propagates through the specimen in the thickness direction to the rear surface. The frequency of temperature wave is selected by considering the thermal diffusion length defined as $\mu = 1/k = (\omega/2\alpha)^{-1/2}$ of the specimen, as to get the thermally thick condition. The ac electric power on the heater is selected lower than 15 mW for the minimum temperature increase in the specimen. The temperature variation at the rear surface was detected by the variation of the electrical resistance of the sensor obtained by using a two-phase lock-in amplifier (NF 5160B) as the phase delay and the amplitude decay. Temperature was controlled by the PID temperature controller (Ohkura, EC 5500), and the dc voltage on the sensor and the temperature of the thermocouple were obtained by the digital recorder LR4110 (Yokogawa). The schematic diagram of the experimental arrangement for TWA is shown in Fig. 1 (b).

2.2.2. Analysis

Assuming the one-dimensional heat flux, temperature wave generated on the front surface ($x = 0$) by ac Joule heating propagates in the thickness direction and is detected by the sensor attached on the rear surface ($x = d$), on which the amplitude decay and the phase delay are observed. The one-dimensional diffusion equation leads to the solution of temperature oscillation $x = d$ as follows [14,15],

$$T(d,t) = \frac{\{j_0 \exp(i\omega t)/(1+i)\}\exp\{-(1+i)kd\}}{[(\lambda k + \lambda_s k_s)^2 - (\lambda k - \lambda_s k_s)^2} \times \exp\{-2(1+i)kd\}]/2\lambda k \qquad k = \sqrt{\frac{\omega}{2\alpha}} \tag{1}$$

where T is ac temperature, t is time, j_0 is heat flux on the heater, λ is thermal conductivity, α is thermal diffusivity and ω is angular frequency of the generated heating wave ($f = \omega/2\pi$). Subscript 's' means the property of backing substrates and the other means the specimen. If the conditions of $kd \gg 1$ or $\lambda k \approx \lambda_s k_s$ are satisfied, the second term in the denominator is much smaller than the first term there, hence Eq. (1) can be

simplified to

$$T(d,t) = \frac{\sqrt{2} j_0 \lambda k \exp(-kd)}{(\lambda k + \lambda_s k_s)^2} \exp\left\{ i\left(\omega t - kd - \frac{\pi}{4}\right)\right\} \quad (2)$$

To note the phase term in Eq. (2), we can get more simple equation as follows,

$$\Delta\theta = -\sqrt{\frac{\omega}{2\alpha}} d - \frac{\pi}{4} \quad (3)$$

where $\Delta\theta$ is the phase delay between the heater and the sensor, and d the specimen thickness. In this equation, the relationship between $\Delta\theta$ and the square root of ω is verified to be a linear one, therefore, when the thickness of the specimen is known, thermal diffusivity α can be obtained from the slope of the plot in ω versus $\Delta\theta$. The Eq. (3) can be rewritten as follows,

$$\alpha = \frac{\pi f d^2}{(\Delta\theta + (\pi/4))^2} \quad (4)$$

By using Eq. (4), α can be determined by $\Delta\theta$ at a fixed frequency. When the temperature is scanned at a constant heating or cooling rate, the thermal diffusivity can be obtained continuously as a function of temperature.

The temperature scan was done in the range from −50 to 20 °C with the temperature scanning rate of 0.5 °C/min in cooling and 0.2 °C/min in heating. The frequency for the temperature scanning measurement was 16 Hz, which was selected by considering the thermally thick condition. During freezing process, the volume expansion is relived to a lateral expansion under the condition for maintaining a constant thickness that can be confirmed by the polarized optical microscope. Even if the thickness expansion was found within 1%, such variation in the thickness would cause the 1% error to the calculated thermal diffusivity value in case of the sample thickness d with 130 μm.

2.3. DSC measurement

Rigaku Thermoflex TAS 200 series DSC 8230D with the cooling instrument was used. Sample (∼2 mg) was sealed in aluminum pan. The heating scanning rate was 2 K/min in the atmosphere of nitrogen. Samples were cooled at 5 K/min before the heating scans. Here the liquid nitrogen was used as the cooling agents.

2.4. XRD–DSC measurement

XRD–DSC (Rigaku XRD–DSC) measurement was undertaken for the simultaneous measurement of X-ray diffractometer and DSC for the study of crystalline structure of eutectic of alkali chloride and ice [19,20]. The specimen of aqueous solution about 10 mg was packed in an aluminum square-shaped container without mechanical grinding. The XRD–DSC operating conditions were as follows: Cu Kα X-ray source, graphite monochrometer, X-ray condition 50 KV 40 mA, divergence slit 0.5°, scattering slit 0.5°, receiving slit 0.3 mm, 5–40° 2θ range, 10°/min speed, 2 K/min heating rate. Nitrogen was used as atmospheric condition. The calibration of θ and 2θ was performed as usual by using a silicon standard. Temperature calibration of DSC was performed as usual using 2–3 mg of highly pure metal chips of Ga, In, Sn and Pb.

3. Results and discussion

Fig. 2 shows the thermal diffusivity of 0.154 M aqueous sodium chloride solution during the cooling and the heating processes between −50 and 20 °C. After a super cooling phenomenon, a steep increase of thermal diffusivity was observed as two steps at −10 and −33 °C, corresponding to the crystallization of pure water and the eutectic formation of sodium chloride and ice, respectively. While in the heating scan, a two-step decreasing of thermal diffusivity was observed at −22.1 and −1.5 °C, also corresponding to the eutectic melting (literature value ca. −21.6 °C) [21] and the depressed melting of ice, respectively. The eutectic composition is approximately 23.6% w/w of sodium chloride, existing as a hydrate of $NaCl{\cdot}2H_2O$ below this temperature [18].

Thermal diffusivity in the heating process of pure water and the aqueous sodium chloride solutions with various concentrations from 0.05 to 4.0 M are shown in Fig. 3. It is obviously seen that for each aqueous solution, thermal diffusivity changes in two steps. The first steep descent of thermal diffusivity corresponds to the eutectic melting of $NaCl{\cdot}2H_2O$, at −22.1 °C, while the second steep descent corresponds to the melting of ice. Both of these changes are strongly depending on the concentration of solute, the higher the concentration of sodium chloride, the higher the decreasing of thermal diffusivity in the eutectic melting. Near to the eutectic concen-

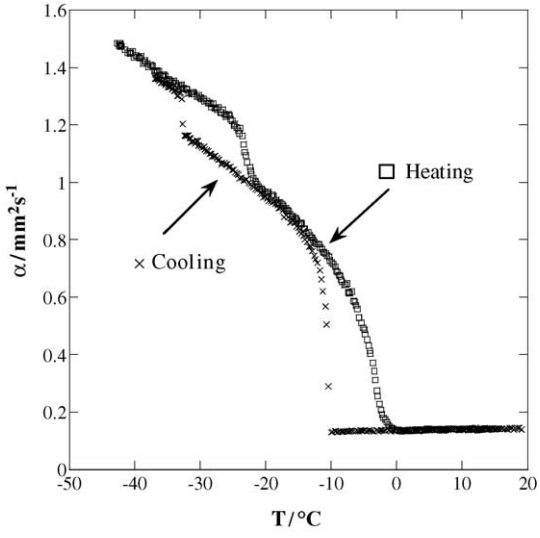

Fig. 2. Thermal diffusivity of aqueous 0.154 M NaCl solution in the cooling (×) and heating (□) processes.

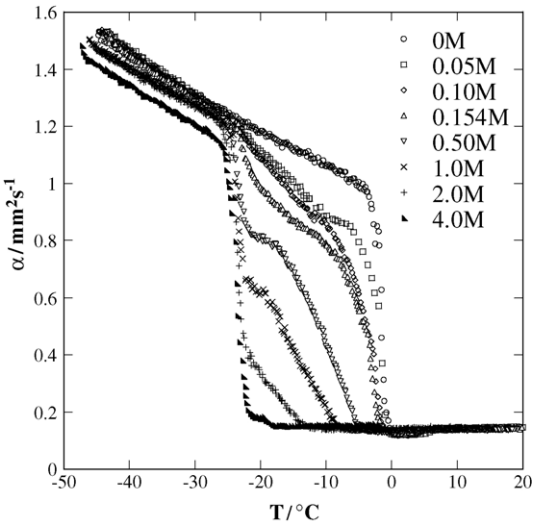

Fig. 3. Thermal diffusivity of aqueous NaCl solutions with various molar concentrations during heating process: (◯) pure water; (□) 0.05 M; (◊) 0.10 M; (△) 0.154 M; (▽) 0.50 M; (×) 1.0 M; (+) 2.0 M; (◣) 4.0 M.

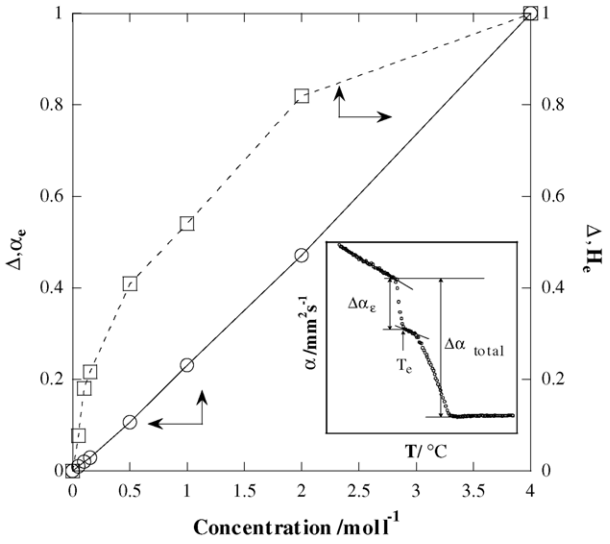

Fig. 4. Thermal diffusivity changing ($\Delta'\alpha_e$) and heat of fusion ratio ($\Delta'H_e$) in the melting of eutectic NaCl·2H$_2$O formed in aqueous NaCl solutions with various molar concentrations: (□) $\Delta'\alpha_e$; (◯) $\Delta'H_e$. Inset shows the determination of T_e, $\Delta\alpha_e$ and $\Delta\alpha_{total}$.

tration (4.03 M), only the first descent of thermal diffusivity was observed at 4.0 M aqueous solution of sodium chloride. On the contrary, the changing of the thermal diffusivity in the melting of ice decreases with the increasing concentration of the aqueous sodium chloride solution. The depression of the melting point (which is corresponding to the liquidus phase boundary in the phase diagram [22]) was clearly observed in the melting area of ice. Below the eutectic melting temperature, the thermal diffusivity increases with the falling of temperature, and higher the solute concentration, lower the value. On the other hand, in the liquid state, each solution with various concentrations shows approximately the same value as that of pure water. The thermal diffusivity in the liquid state slightly increases with increasing the temperature.

The change ratio of thermal diffusivity $\Delta'\alpha_e$ ($\Delta\alpha_e/\Delta\alpha_{total}$) and that of heat of fusion by DSC $\Delta'H_e$ ($\Delta H_e/\Delta H_{total}$) due to the melting of eutectic was shown in Fig. 4, plotted against the concentrations of aqueous sodium chloride solution. Here, $\Delta\alpha_e$ and $\Delta\alpha_{total}$ are the change of thermal diffusivity during the eutectic melting and the total change of thermal diffusivity from the solid to the liquid state, respectively. The schematic determination of $\Delta\alpha_e$, $\Delta\alpha_{total}$ and T_e were shown schematically in the inset of Fig. 4. ΔH_e and ΔH_{total} are the heat of fusion for the eutectic and the total heat of fusion of the aqueous alkali chloride system, respectively. $\Delta'\alpha_e$ and $\Delta'H_e$ increase with the increasing concentration, because the amount of the eutectic crystalline increases with the increasing concentration of NaCl solute. However, the concentration dependence of $\Delta'\alpha_e$ and $\Delta'H_e$ was different. The increase of $\Delta'H_e$ tends to be linear, while for $\Delta'\alpha_e$, the increase tendency occurs to be the curved line with the increasing concentration. At lower concentration, the rise of $\Delta'\alpha_e$ is remarkably larger than that of $\Delta'H_e$. In other words, thermal diffusivity is much more sensitive to detect the change in highly structure of coexistence of eutectic and ice.

Fig. 5 shows the thermal diffusivity of aqueous KCl solutions with various concentrations in the heating process. The melting temperature of the eutectic (T_e) of KCl and ice is −10.4 °C, higher than that of NaCl solution. In the KCl solutions, thermal diffusivity in the frozen state has the larger variation depending on the solute concentration than that observed in the NaCl solutions, the higher the concentration, much lower the thermal diffusivity value, and the thermal diffusivity also changes in two descent steps in the heating scan. For the KCl solution with the concentration higher than

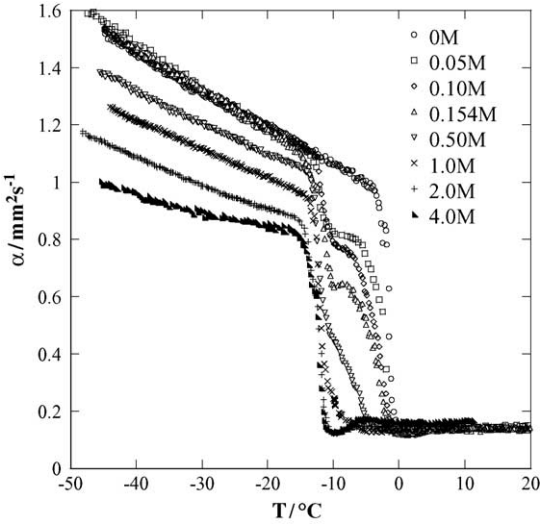

Fig. 5. Thermal diffusivity of aqueous KCl solutions with various molar concentrations during heating process: (◯) pure water; (□) 0.05 M; (◊) 0.1 M; (△) 0.154 M; (▽) 0.50 M; (×) 1.0 M; (+) 2.0 M; (◣) 4.0 M.

Table 1
Melting temperature for the eutectic crystallization (T_e) of alkali chlorides

T_e	NaCl	KCl	RbCl	CsCl
From literature [18]	−21.7	−10.4	−16.0	−23.0
From TWA technique	−22.1	−10.8	−16.4	−23.3

2.0 M, only one step decrease of thermal diffusivity was observed, in which only the eutectic melting occurred. For other kinds of alkali chloride solutes such as RbCl and CsCl, the same experiments were performed, and the two-step descents of thermal diffusivity were also found in the heating scan. The melting temperatures (T_e) of these four kinds of the eutectics determined by TWA (as shown in the inset of Fig. 4) were shown in Table 1 together with the literature values [18]. The temperatures obtained from TWA method agree well with the literature value.

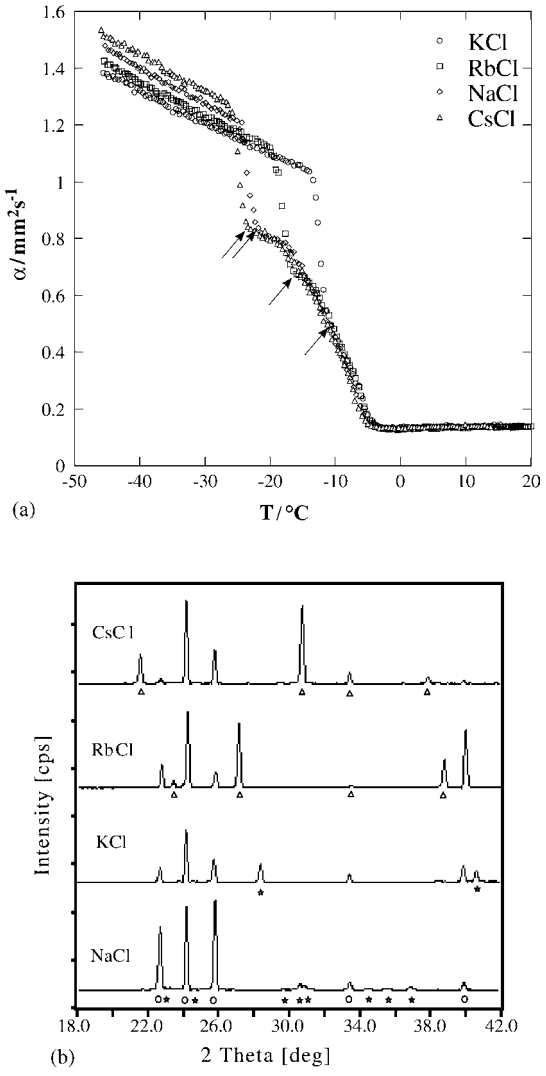

Fig. 6. (a) Thermal diffusivity of 0.5 M aqueous alkali chloride solutions during heating process, (◯) KCl; (□) RbCl; (◊) NaCl; (△) CsCl. (b) X-ray diffraction patterns for 0.5 M aqueous alkali chloride solutions taken at −40 °C.

Fig. 6a depicted the thermal diffusivity of these four kinds of the aqueous solutions with the concentration of 0.5 M in the heating scan, in which the eutectic melting temperature of each alkali chloride solute was clearly observed by the steep descent of thermal diffusivity. Thermal diffusivities below −30 °C are in the order of the eutectic melting temperature, the higher the eutectic melting temperature (KCl > RbCl > NaCl > CsCl), the lower the thermal diffusivity value (CsCl > NaCl > RbCl > KCl). Here we should pay attention to the value of thermal diffusivity at which the eutectic complete its melting, as pointed out with the arrows in Fig. 6(a). Thermal diffusivity values occurred in such regions different remarkably from each other. As we know, thermal diffusivity values in such regions contribute to the ice and the concentrated aqueous solution. As shown in the former figures, the thermal diffusivity of ice is about 10 times as that of aqueous solution, so the different thermal diffusivity value at the arrow points for each solution is deduced mainly from the different amount of ice [10,23,24]. It was well known that the eutectic is composed of solute and ice, and the knowable example of eutectic of $NaCl{\cdot}2H_2O$, is composed of one molecular NaCl and two molecules of water. In the freezing process of aqueous NaCl solution, the water in the aqueous solutions would turn into ice gradually and finally the remained water would combine to the NaCl and form the eutectic crystallization. For other solutes such as KCl, RbCl and CsCl, the number of water bound to each solute was not given in the earlier literature, but it is suggested that the amount of water bound to each solute is different from each other, the largest in KCl and the smallest in CsCl aqueous solutions.

X-ray diffraction patterns recorded at −40 °C for these four kinds of aqueous solutions with the concentration of 0.5 M were shown in Fig. 6(b). For each solution, the angles of relatively high intensity peaks occurred are different from each other. While the angles which were marked with circle at 22.8°, 24.3°, 26.2°, 33.6° and 40.2° were demonstrated to be the ice, for the angles of relatively high intensity peaks due to ice are 22.8°, 24.3°, 26.2°, 33.6°, 40.1°, 43.7° and 47.3° as defined by Joint Committee on Powder Diffraction Standard (JCPDS) file no.16-687 [25]. For aqueous NaCl solution and aqueous KCl solution, the relatively high intensity peaks appeared at other angle regions which were marked with star are all corresponding well to those defined by JCPDS file no. 29-1197 and no. 04-587, respectively, which were all confirmed to be the eutectic formed in the corresponding frozen solutions, respectively. Although for the eutectic formed in frozen state of aqueous solutions of RbCl and CsCl, there does not exist any literature reference on the X-ray diffraction pattern, here we still confirm that the peaks appeared at other angle region which marked with triangle are owing to the eutectic crystallization from the simultaneous measurement of DSC. Because in heating measurement from −50 to 25 °C, all the peaks marked with triangles disappeared after the eutectic melting, and then the residual peaks are all corresponding to that of ice.

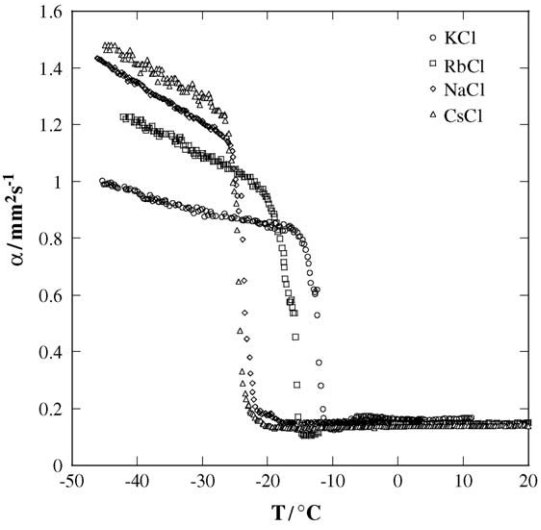

Fig. 7. Thermal diffusivity of 4.0 M aqueous alkali chloride solutions during heating process: (◯) KCl; (□) RbCl; (◊) NaCl; (△) CsCl.

Fig. 7 shows the thermal diffusivity of four kinds of aqueous alkali chloride solutions with the concentration of 4.0 M. There only exists one steep descent in the changing of thermal diffusivity in the heating process. In other words, for these aqueous solutions only the eutectic formed in the frozen state. It is obviously seen that below −20 °C the thermal diffusivity value of the eutectic of KCl is the lowest, next is that of RbCl and NaCl, the largest one is that of CsCl, the same order as observed in Fig. 6(a).

Fig. 8 shows the values of thermal diffusivity for these four kinds of aqueous solutions at −40 and 10 °C as a function of concentration. In the liquid state, thermal diffusivity of each solution shows small difference with pure water at about 0.142 $mm^2\ s^{-1}$ (10 °C). In the frozen state, thermal diffusivities for each solution with the concentration lower than 0.154 M are the same at about 1.4 $mm^2\ s^{-1}$. On the other hand in the concentrations higher than 0.154 M up to 4 M, thermal diffusivity shows a large difference depending on the different alkali chloride solutes. Thermal diffusivity of aqueous CsCl solution seems to be nearly to that of ice. While for aqueous KCl solution, thermal diffusivity shows strong dependence on the concentration, and it keeps the lowest one comparing with other kinds of aqueous solutions at the same concentration. This is due to the low fraction of ice and the low thermal diffusivity value of eutectic of KCl. Thermal diffusivity in the frozen state is closely correlated with the highly structure of coexistence system of eutectic and ice, depending on the solute of alkali chloride.

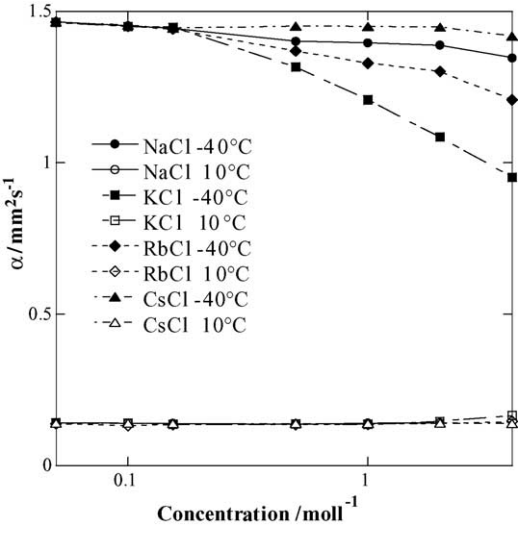

Fig. 8. Thermal diffusivities for aqueous alkali chlorides solutions with various molar concentrations at −40 and 10 °C: (●) NaCl at −40 °C; (◯) NaCl at 10 °C; (■) KCl at −40 °C; (□) KCl at 10 °C; (♦) RbCl at −40 °C; (◊) RbCl at 10 °C; (▲) CsCl at −40 °C; (△) CsCl at 10 °C.

4. Conclusion

Temperature wave analysis technique was applied to measure the thermal diffusivity of aqueous solutions of alkali chloride with various concentration in a continuous temperature scan over the temperature range including the freezing–thawing processes of ice and eutectic.

Thermal diffusivity drastically changes in the melting of eutectic and ice during the heating process. In the unfrozen state, there does not exist any obvious difference in the thermal diffusivity among the four kinds of aqueous alkali chloride solutions. In the frozen state, however, thermal diffusivity is strongly depending on the concentration and the kinds of the alkali chloride solute. Thermal diffusivity is sensitive to detect the subtle change in the eutectic melting comparing with that captured by DSC method.

Potassium chloride, rubidium chloride, sodium chloride and cesium chloride are all form eutectic with ice, and the eutectic melting temperatures are different from each other, it is independent of the radius of the alkali ion. Thermal diffusivity in the frozen state shows a variation depending on the kind of alkali chloride solute, the higher the thermal diffusivity, the lower the eutectic temperature. It suggests the different water bonding ability in the composition of different kind eutectic.

The advantage of TWA is that it not only permits unambiguous identification of the thermal diffusivity value, but also provides a thermal understanding of the alterations in the solid-state occurred during the heating process. It is thought that these results are sensitive to the structural change due to the phase transition.

References

[1] J. Kestin, I.R. Shankland, Int. J. Thermophys. 5 (1984) 241.
[2] F.H. Horne, B.K. Borey, Int. J. Thermophys. 7 (1986) 87.
[3] A.A. Minakov, Yu.V. Bugoslavsky, C. Schick, Thermochim. Acta 317 (1998) 117.

[4] A.A. Minakov, C. Schick, Thermochim. Acta 330 (1999) 109.
[5] A.A. Minakov, S.A. Adamovsky, C. Schick, Thermochim. Acta 403 (2003) 89.
[6] D. Dadarlat, K.J. Riezebos, D. Bicanic, C. van den Berg, E. Gerkema, V. Surducan, Adv. Food Sci. 20 (1998) 27.
[7] D. Dadarlat, J. Gibkes, D. Bicanic, A. Pasca, J. Food Eng. 30 (1996) 155.
[8] J. Caerels, C. Glorieux, J. Thoen, Rev. Sci. Instrum. 71 (2000) 3506.
[9] N. Hamdami, J.Y. Monteau, A.L. Bail, Food Res. Int. 37 (2004) 703.
[10] R. Pongsawatmanit, O. Miyawaki, T. Uyano, Biosci. Biotechnol. Biochem. 57 (1993) 1072.
[11] Y. Nagasaka, A. Nagashima, Rev. Sci. Instrum. 52 (1981) 229.
[12] A. Alloush, W.B. Gosney, W.A. Wakeham, Int. J. Thermophys. 3 (1982) 225.
[13] Y. Nagasaka, T. Hatakeyama, M. Okuda, A. Nagashima, Rev. Sci. Instrum. 59 (1988) 1156.
[14] T. Hashimoto, A. Hagiwara, A. Miyamoto, Thermochim. Acta 163 (1990) 317.
[15] T. Hashimoto, J. Morikawa, T. Kurihara, T. Tsuji, Thermochim. Acta 299 (1997) 95.
[16] J. Morikawa, S. Yamamoto, N.J. Chen, T. Hashimoto, Netsu Sokutei 29 (2002) 27.
[17] J. Morikawa, N.J. Chen, K. Yukiko, T. Hashimoto, The Sixteenth European Conference on Thermophysical Properties, London, 2002, p. 245.
[18] S. Fujiwara, Y. Nishimoto, Anal. Sci. 14 (1998) 507.
[19] T. Arii, A. Kishi, Y. Kobayashi, Themochim. Acta 325 (1999) 151.
[20] A. Kishi, M. Otsuka, Y. Matsuda, Colloid Surf. B: Biointerfaces 25 (2002) 281.
[21] L. Rey, Ann. N.Y. Acad. Sci. 85 (1960) 510.
[22] Landolt-Bornstein, Physikalisch-chemische Tabellen, Auflage 1, vol. 5, Springer-Verlag, Berlin, 1923.
[23] R. Pongsawatmanit, O. Miyawaki, Biosci. Biotechnol. Biochem. 57 (1993) 1650.
[24] O. Miyawaki, R. Pongsawatmanit, Biosci. Biotechnol. Biochem. 58 (1994) 1222.
[25] K. Kajiwara, A. Motegi, N. Murase, CryoLetters 22 (2001) 311.